

Symmetries and modelling functions for diffusion processes

A.G. Nikitin^a, S.V. Spichak^a, Yu. S. Vedula^b and A.G. Naumovets^b

^a*Institute of Mathematics of National Academy of Sciences of Ukraine,
3 Tereshchenkivs'ka Street, Kyiv-4, Ukraine, 01601
e-mail: nikitin@imath.kiev.ua;*

^b*Institute of Physics of National Academy of Sciences of Ukraine,
46 Prospect Nauki, Kyiv-28, Ukraine, 03028
e-mail: naumov@iop.kiev.ua*

Short title: Symmetries and modelling functions

PACS numbers: 68.43.Jk - Diffusion of adsorbates; 66.30.Dn - Theory of diffusion and ionic conduction in solids.

Abstract

A constructive approach to theory of diffusion processes is proposed, which is based on application of both the symmetry analysis and method of modelling functions. An algorithm for construction of the modelling functions is suggested. This algorithm is based on the error functions expansion (ERFEX) of experimental concentration profiles. The high-accuracy analytical description of the profiles provided by ERFEX approximation allows a convenient extraction of the concentration dependence of diffusivity from experimental data and prediction of the diffusion process. Our analysis is exemplified by its employment to experimental results obtained for surface diffusion of lithium on the molybdenum (112) surface pre-covered with dysprosium. The ERFEX approximation can be directly extended to many other diffusion systems.

1 Introduction

Experimental and theoretical studies of diffusion processes are of a great importance for various branches of physics, biology, chemistry and other natural sciences. In addition, such studies have important applications in medicine and many technological processes. A special interest is excited by surface diffusion processes which appear in many physical and chemical systems. In particular, they are used in various kinds of nanotechnologies.

The theory of diffusion processes started in 1855 when Fick derived his classical diffusion equation [1]

$$\frac{\partial \theta}{\partial t} - \frac{\partial}{\partial x_a} \left(D \frac{\partial \theta}{\partial x_a} \right) = 0, \quad (1)$$

which still is a corner stone of the diffusion theory. In equation (1) D is a diffusion coefficient, in general case depending on species concentration θ , and x_a with $a = 1, 2, 3$ are spatial variables (summation over the repeated indices a is imposed). Being supplemented by an appropriate initial data, equation (1) serves as a background for description of such diffusion processes which are characterized by diffusion flows linear in concentration gradients and not depending explicitly on space and time variables.

Two standard problems of a diffusion theory are:

- 1) To describe time evolution of the diffusion process, and
- 2) To specify the dependence of the diffusion coefficient on concentrations of diffusing species.

Of course, these problems are closely related, since if we know how the diffusion coefficient depends on concentration θ , then the time evolution of the corresponding diffusion process can be found using the Fick equation (1) and the related initial data. On the other hand, if we know θ as a function of time variable t and spatial variables x_a , then we can find D solving the inverse diffusion problem using again equation (1).

Both mentioned problems are very complicated and in general need rather sophisticated techniques. Even if we know the diffusion coefficient as an explicit function of concentration, then generally speaking it is possible to find only an approximate (numerical) solution of the first problem if at all. The second problem has a much more complex character, but in the case of a sharp step-like initial θ profile it is possible to use the Boltzmann-Matano (BM) approach [2] and reconstruct the concentration dependence $D(\theta)$ of the diffusion coefficient. This approach enables one to make a numerical calculation of the diffusion coefficient, but its accuracy is not very high, especially for small and large concentrations θ .

Experimental data and numerical solutions are very important for description of a diffusion process, but to formulate its theory it is desirable to create some analytical expressions for studied values. Unfortunately, there are only few known exactly solvable realistic diffusion problems, the most famous of them is probably the Barenblatt one [3]. Thus it is a common practice to use rather rough analytic presentations of $D(\theta)$ to make a qualitative analysis of diffusion process (see, e.g., [4]).

In the present paper we propose a new method for description of time evolution of a diffusion process and calculation of the diffusion coefficient. The distinct feature of our approach is that we find both functions $\theta = \theta(t, x)$ and $D = D(\theta)$ in an explicit form, i.e., solve both problems 1) and 2) analytically. To achieve this goal we start with experimental data for a particular diffusion system and make the error functions expansion (ERFEX) of concentration profiles. Analytic description of diffusion processes is very convenient for their qualitative analysis. Moreover, our description appears to be rather good quantitatively also; its deviation from experimental data does not exceed the inaccuracy of measurements.

We apply this approach to describe in detail the surface diffusion of Li deposited on the molybdenum (112) surface which had been previously covered with a submonolayer of dysprosium. One more process, the diffusion of Dy adsorbed on Mo(112), is used to examine the method generality. Moreover, we believe that it can have a much wider application area.

2 Experimental data and symmetries

Let us start with experimental data representing surface diffusion of Li on the Mo(112) surface precovered with a 0.25 monolayer of dysprosium (below we designate it as Dy-Mo(112) surface). The data were obtained in ultra-high vacuum using local measurements of the work function by a contact potential method (see [5]-[7] for details).

A schematic sketch of the method, termed scanning contact potential microscopy, is shown in Fig. 1. At the beginning of the experiment, we uniformly covered the

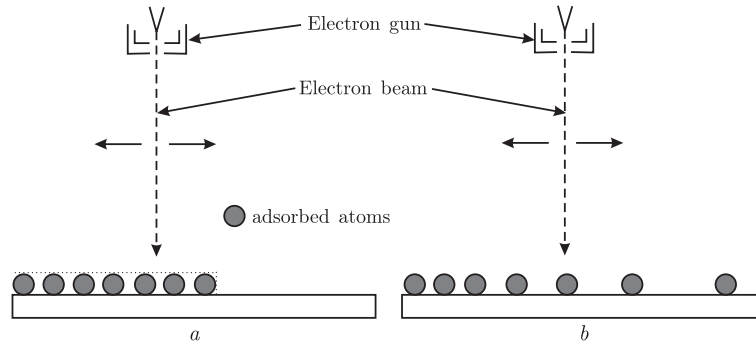


Figure 1: Probing the surface distribution of adatoms by scanning contact potential microscopy. (a) The initial step-like adatom distribution. (b) The adatom distribution after surface diffusion.

clean surface of a (112) oriented Mo single crystal with dysprosium (its surface density amounted to 0.25 of a monoatomic layer) and equilibrated it by annealing at $T=1100$ K. The Dy adatoms served thereafter as a controllable admixture which could affect the diffusion kinetics of lithium [6]. Then, using a semiplane mask (screen) placed between the Li evaporator and the prepared substrate, a half of the crystal surface

was covered at room temperature with Li while its another half remained clean of Li (Fig. 1,a). The surface was scanned with an electron beam formed by an electron gun. The movable beam was used to record the distribution of the contact potential (work function) over the sample surface by P.A. Anderson's (retarding field) method. In separate experiments, the work function change was carefully calibrated with respect to the absolute surface concentration of adsorbed atoms (adatoms). The calibration data served to convert the work function values to adatom concentrations, n . To characterize the relative concentration of adatoms with respect to substrate surface atoms, we shall use, as it is conventional in surface science, the term "degree of coverage" (or, for short, "coverage"). It is defined as $\theta = n/n_M$, where n_M is the concentration of the substrate surface atoms ($n_M = 8.3 \cdot 10^{14} \text{cm}^{-2}$ for the Mo(112) surface). The coverage $\theta = 1$ is usually termed the geometrical monolayer.

Under the experimental conditions provided in [5, 6, 7], there was neither evaporation of the adsorbate into vacuum nor its diffusion (drain) into volume of the Mo substrate. Thus the experimental results relate to a case a "pure" surface diffusion which could be described by equation (1). Notice that the length of the crystal sample along the diffusion direction was about 10 mm while the extension of the diffusion zone in the experiments did not exceed 1.2-1.5 mm. Thus the boundary effects connected with the finite size of the sample could be neglected

The initial Li distribution was step-like shaped. Then upon heating the adsorbate profile spreads out due to surface diffusion. Since the edge of the step was oriented normally to the atomic channels on the Mo(112) surface, the diffusion proceeded quasi-one-dimensionally along the channels, i.e. along the $[\bar{1}, \bar{1}, 1]$ direction [5-7].

The experiment consisted of a series of measurements in which we recorded the time evolution of the coverage profiles due to diffusion at a constant annealing temperature. At the beginning of each experiment ($t=0$), a standard (step-like) initial coverage profile of the adsorbate was created and recorded on the crystal kept at room temperature, at which the adatom mobility is negligible. This profile is labeled $t=0$. Then the crystal sample was annealed at a fixed temperature. From time to time, the annealing was interrupted and the crystal quickly cooled down to room temperature to record a new coverage profile arising due to diffusion. After that the annealing was continued, and so on. In this way we obtained a series of profiles corresponding to different annealing times and a constant annealing temperature. Such experiments could be repeated at different annealing temperatures to determine the temperature dependence of the diffusion kinetics.

Measurements were made at times $t = 0, 1200, 2100, 3600$ and 5400 (seconds) at stable temperature $T = 600K$, experimental error in θ was $\Delta\theta = 0.003$. The recorded coverage profiles are presented in Fig. 2.

The initial profile ($t = 0$) is step-like shaped, but technologically it was impossible to form an ideal step. The profiles obtained as a result of surface diffusion have a common intersection point at $x = 0.88, \theta = 0.192$ and have rather smooth contours. Moreover, a convention is used to set $\theta = 0$ in the region where its value is below the

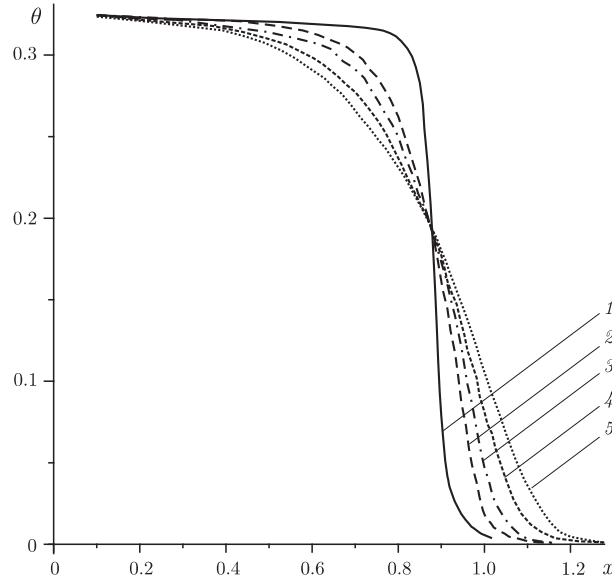


Figure 2: Coverage profiles of Li adsorbed by Dy-Mo(112) at T=600 K: initial, $t = 0$ (1), and measured at $t = 1200$ s (2), $t = 2100$ s (3), $t = 3600$ s (4), $t = 5400$ s (5). The x - coordinate gives distance in mm.

measurement accuracy.

Our task is to give a phenomenological theory of the related diffusion process. Abstracting from complicated underlying physical effects which are discussed in paper [8], we will describe the time evolution of the diffusion process and derive the dependence of the diffusion coefficient on concentration.

To achieve our goal, we will exploit symmetries which form the integral part of diffusion processes. A precise analysis of the experimental data makes it possible to find a specific symmetry which characterizes coverage profiles. Namely, let us fix a profile θ recorded at time t and consider it as a given function of x . Then any other profile θ' measured at time t' can be obtained from θ using the following transformation:

$$x \rightarrow x' = (x - x_0)\sqrt{\frac{t}{t'}} + x_0, \quad (2)$$

where $x_0 = 0.88$ is coordinate of the point common for all coverage profiles.

This statement can be verified directly or using computer fits to the experimental curves. For example, starting with experimental data for $t = 3600$ s and applying transformation (2), one can reproduce profiles for $t = 1200$ s, 2100 s and 5400 s.

It should be stressed that the found symmetry is rather exact. As a rule, a deviation of curves obtained using transformation (2) from experimentally measured profiles is within the limits of experimental error, and this deviation decreases with growing time. For example, comparing experimental data for coverage profile at

$t = 5400$ s (Fig. 2) and the corresponding values obtained via change (2) we conclude that they are very similar, namely, the differences are below the experimental error.

3 Time evolution derived from symmetries

The exact meaning of the symmetries discussed in Section 2 is that functions $\theta(t, x)$ describing coverage profiles are invariant with respect to the following one-parametric group of transformations:

$$t \rightarrow t' = e^{2\alpha}t, \quad x \rightarrow x' = xe^\alpha + x_0(1 - e^\alpha), \quad (3)$$

where α is a real parameter. Indeed, solving the first of equations (3) for e^α and using the second equation we come to relations (2).

Starting with (3) and using tools of the classical group analysis, it is possible to describe time evolution of profile $\theta(t, x)$. Indeed, the infinitesimal operator of transformations (3) has the form:

$$X = \eta \frac{\partial}{\partial t} + \xi \frac{\partial}{\partial x} \equiv 2t \frac{\partial}{\partial t} + x \frac{\partial}{\partial x} - x_0 \frac{\partial}{\partial x},$$

where $\eta = \frac{\partial t'}{\partial \alpha}|_{\alpha=0}$ and $\xi = \frac{\partial x'}{\partial \alpha}|_{\alpha=0}$ [9]. The invariance of coverage profiles with respect to transformations (3) means that $\theta(t, x)$ solves the following equation [9]:

$$X\theta(t, x) = 0. \quad (4)$$

It follows from (4) that time evolution of coverage profiles $\theta(t, x)$ is described by the following equation:

$$\frac{\partial \theta}{\partial t} = \frac{x - x_0}{2t} \frac{\partial \theta}{\partial x} \quad \text{or} \quad \frac{\partial \tilde{\theta}}{\partial t} = \frac{y}{2t} \frac{\partial \tilde{\theta}}{\partial y}, \quad (5)$$

where $y = x - x_0$, $\tilde{\theta}(t, y) = \theta(t, y + x_0)$. As an initial condition we can choose one of measured profiles, say that one which corresponds to $t = t_2 = 1200$:

$$\tilde{\theta}(t_2, y) = \theta_2 = \theta_2(y + x_0) \quad (6)$$

where $\theta_2(x)$ is a function given numerically in Table 1. Henceforth we omit tilde and write $\theta(t, y)$ instead of $\tilde{\theta}(t, y)$.

Thus we can describe the time evolution of the coverage profiles without a diffusion equation. Solving problem (5) with condition (6) and using numerical data given in the Appendix we can find shapes of these profiles for any time. Some of such profiles are presented in Fig. 3.

As we see, the very existence of the symmetries in experimental data makes it possible to predict shapes of the coverage profiles which will appear at various times

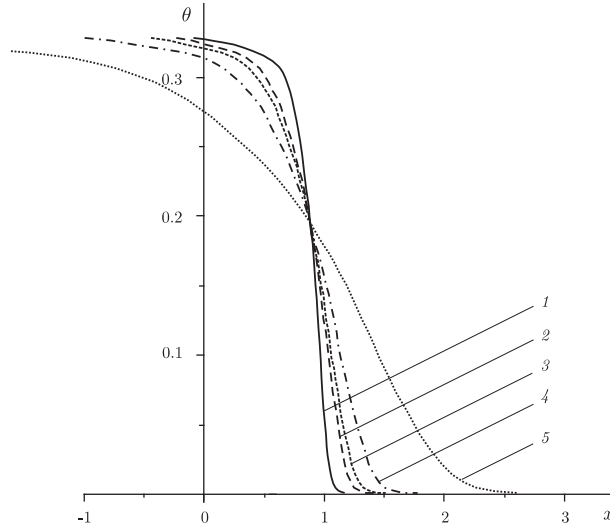


Figure 3: Coverage profiles $\theta(t, x)$ for Li on Dy-Mo(112) at T=600 K: experimental for $t = 2100$ s (1) and theoretical for $t = 7000$ s (2), 10000 s (3), 20000 s (4), 100000 s (5). The x -coordinate gives distance in mm.

of heating. This statement is valid for any diffusion system which admits symmetries (3). But if we are interested in analytical description of the diffusion process, we have to pose initial conditions analytically. A basic problem is to create a consistent model of the diffusion process, i.e. find the dependence of the diffusion coefficient on concentration, which is important for physical interpretation.

In the following sections we solve this problem and give explicit representations of coverage profiles $\theta(t, x)$ in analytical form.

4 Symmetries of diffusion models

Transformations (2) have a stable point $x = x_0 = 0.88$ and $\theta = 0.194$ which was the only one not being changed. It is convenient to choose just x_0 as a zero point of our coordinate system, i.e. to use variable $y = x - x_0 = x - 0.88$ instead of x .

Taking into account that in fact we deal with a process which is one-dimensional with respect to spatial variables, it is possible to reduce equation (1) to the following form:

$$\frac{\partial \theta}{\partial t} - \frac{\partial}{\partial y} \left(D \frac{\partial \theta}{\partial y} \right) = 0 \quad (7)$$

where $D = D(\theta)$, $y = x - x_0$.

Formula (7) represents a rather complicated non-linear partial differential equation. In addition, we do not know the θ -dependence of the diffusion coefficient D .

Fortunately, this equation has a very useful symmetry with respect to scaling of independent variables, being invariant with respect to transformations (3), or

$$t \rightarrow t' = e^{2\alpha}t, \quad y \rightarrow y' = ye^\alpha, \quad \theta \rightarrow \theta' = \theta. \quad (8)$$

Just this nice property of the diffusion equation makes it possible to use the Boltzmann variable $\xi = \frac{y}{\sqrt{t}}$ and search for its similarity solutions $\theta = \theta(\xi)$ where both θ and ξ are invariants of transformations (8).

Notice that equation (7) is invariant also with respect to shifts of independent variables

$$t \rightarrow t + b, \quad y \rightarrow y + k \quad (9)$$

with arbitrary real parameters b and k . This invariance allows one to choose arbitrary initial time and justifies the transition from x to y which we made above. For some particular functions $\tilde{D}(\theta)$, symmetry of the Fick equation is more extended. A complete classification of symmetry groups of equation (7) has been made by Ovsiannikov [10], a complete group classification of systems of two diffusion equations with source terms can be found in [11] and [12].

However, symmetries (8) should be compatible also with the initial data of our problem, which are of the form:

$$\theta(0, y) = \theta_1(y), \quad (10)$$

where θ_1 is the initial coverage profile ($t = t_1 = 0$) represented numerically in the Appendix and graphically in Fig. 2.

We see that the experimentally created profile at $t = 0$ is not strictly step-shaped, and so *is not invariant with respect to scaling* (8). However, the profile θ_1 is not far from a step and can be considered as a perturbed Heaviside function $H(-y)$ multiplied by 0.327 ($\theta_{max} = 0.327$ is the maximum coverage in the initial θ profile). On the other hand, and it is an experimental fact, for sufficiently large times t solutions of our problem indeed are invariant with respect to transformations (2). And if we apply this transformation to infinitely small t' , all profiles $\theta_1, \theta_2, \dots, \theta_4$ tend to a step-shaped one. So we have a direct experimental confirmation of the known mathematical fact that similarity solutions of the diffusion equation (7) can serve as attractors for other solutions. In other words, the yet unknown diffusion coefficient should depend on θ in such a way that the related Cauchy problem (7), (10) be asymptotically stable with respect to small perturbations of the initial data (see [13] for exact definitions).

Thus, instead of the actual initial data presented in the Appendix and Fig. 2, we can consider an idealized situation when the initial coverage has a step shape, and to suppose that for $t = 0$ the concentration is proportional to the Heaviside function $H(-y)$:

$$\theta(0, y) = \theta_{max} \cdot H(-y) = \begin{cases} 0.327, & y < 0, \\ 0, & y \geq 0 \end{cases} \quad (11)$$

where $\theta_{\max} = 0.327$ is the maximum concentration in the initial coverage profile.

The initial-value problem (7), (11) is invariant with respect to transformations (8), and so it is possible to search for invariant solutions $\theta = \theta(\xi)$ depending on invariant variable $\xi = \frac{y}{\sqrt{t}}$. In this way the problem is reduced to the following one:

$$\begin{aligned} \xi \frac{\partial \theta}{\partial \xi} + 2 \frac{\partial}{\partial \xi} \left(D \frac{\partial \theta}{\partial \xi} \right) &= 0, \\ \theta(-\infty) &= 0.327, \quad \theta(+\infty) = 0. \end{aligned} \tag{12}$$

Remember that we do not know yet the dependence of the diffusion coefficient D on degree of coverage θ . Using experimental data describing dependence of θ on x at fixed heating time t and applying the BM approach [2] it is possible to calculate D numerically. Unfortunately, such calculations cannot be done with a sufficiently good accuracy, especially in the region of small concentrations. In addition, in this way we cannot find the diffusion coefficient in an analytical form. In Section 6 we suggest another approach which presupposes direct analytical modelling of profiles $\theta(\xi)$.

5 Generalized diffusion equation

Thus we had formulated a possible model of the analyzed diffusion process which is based on equation (7) whose solutions should satisfy the idealized initial conditions (11). However, the possibility of using Fick equation (7) is nothing but a supposition which needs additional justifications. In particular, it is necessary to be ensured that the diffusion flow is linear in the concentration gradient.

However, we can use the well justified fact, i.e., the invariance of experimental coverage profiles with respect to transformations (2), and set the following problem: to find the most general evolution equation which is compatible with this symmetry.

Thus let us suppose that the evolution equation admits symmetries (2) and also shifts (9) (i.e., does not depend explicitly on space and time variables). Then using tools of classical Lie analysis [9], we easily find its general form:

$$\frac{\partial P}{\partial t} - \frac{\partial}{\partial y} \left(\tilde{D} \frac{\partial P}{\partial y} \right) + G \left(\frac{\partial P}{\partial y} \right)^2 = 0 \tag{13}$$

where P is a dependent variable whose evolution we need to describe, \tilde{D} and G are arbitrary functions of P . In particular P can represent a degree of coverage, in this case it should be changed to θ .

We do not present the related routine calculations since our rather strong restrictions (equation should be of evolutionary type and admit the above mentioned symmetries) in fact reduce the problem of deducing of (13) to direct use of the dimension analysis.

Equation (13) is a direct generalization of the Fick equation (7), and the latter corresponds to a particular choice $G = 0$.

Thus starting with symmetries (2), which can be found in the experimental data, and symmetries (9), which are natural transformations for the considered diffusion system, we deduce the generalized diffusion equation (13) which includes the Fick equation (7) as a particular case. Possible physical motivations for generalization of equation (7) to (13) are discussed in Section 10.

6 Modelling functions for coverage profiles

It is well known that in the case when diffusion coefficient D is independent on concentration, the general solution of the problem (7), (11) is given by the following equation:

$$\theta(t, x) = a \operatorname{erfc}(b\xi)$$

where $a = \theta_{\max}/2$, $b = 1/(2\sqrt{D})$, $\xi = x/\sqrt{t}$ and erfc is the complementary error function:

$$\operatorname{erfc}(z) = 1 - \operatorname{erf}(z), \quad \operatorname{erf}(z) = \frac{2}{\sqrt{\pi}} \int_0^z e^{-t^2} dt.$$

This fact suggests using just the error function as a constructive element of concentration profiles for θ -dependent diffusivities. This idea appears to be very successful for description of diffusion processes in general and the processes discussed in Sections 2 and 9 in particular.

In this section we present and discuss examples of modelling functions for the coverage profiles. An algorithm for constructing such functions is given in the following section.

First we consider a rather straightforward representation of profiles $\theta(\xi)$ which, however, is valid only in a reduced interval of the Boltzmann variable ξ :

$$\theta = \theta_{(1)} = a_1(1 - \operatorname{erf}(b_1\xi)^2) \tag{14}$$

where a_1 and b_1 are parameters. Asking for minimal mean-square deviation of function (14) and using MAPLE tools we fix parameters a_1 and b_1 to be

$$a_1 = 0.175, \quad b_1 = 0.375.$$

Function $\theta_{(1)}$ perfectly describes the shape of profile $\theta(\xi)$ for ξ lying in the interval $0.6 < \xi < \infty$, see Fig. 4. In this interval the discrepancy $|\theta - \theta_{(1)}|$ does not exceed inaccuracy of measurements. However, for $\xi < 0.6$ this discrepancy increases.

In order to obtain a modelling function for all non-negative ξ , it is sufficient to add a small extra term to $\theta_{(1)}$ and define:

$$\theta_{(2)} = \theta_{(1)} + a_2 \operatorname{erfc}(b_2\xi), \quad \xi \geq 0 \tag{15}$$

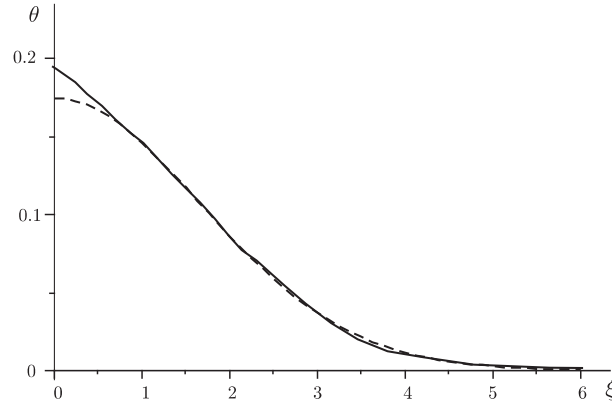


Figure 4: Experimental profile $\theta(\xi)$ for $t = 5400$ (full curve) and the curve θ_1 given by relation (14) (broken curve). Units for ξ are 10^{-3} (mm/s $^{1/2}$)

where $a_2 = 0.02$ and $b_2 = 1.7$.

Function (15) gives a very precise presentation for the profile obtained experimentally at $t = 3600$ s; the deviation $|\theta - \theta_{(1)}|$ does not exceed the inaccuracy of measurements. Fig. 5 presents the experimental curve and curve defined by equation (15), and it is seen that they practically coincide. More exactly, the deviation of values of function (15) from experimental data is less than 0.003.

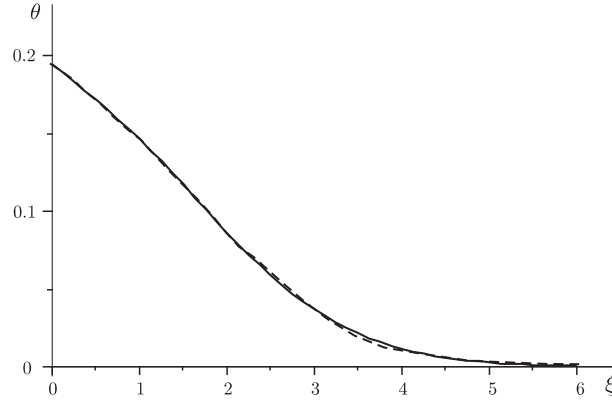


Figure 5: Coverage profiles $\theta(\xi)$: experimental data for $t = 3600$ s (full curve) and function given by relation (15) (broken curve). Units for ξ are 10^{-3} (mm/s $^{1/2}$)

One more possible modelling function is given by the following equation:

$$\theta_{(3)} = a'_1(1 - \text{erf}(b'_1\xi)^3) + a'_2\text{erfc}(b'_2\xi) \quad (16)$$

where $a'_1 = 0.145$, $b'_1 = 0.395$, $a'_2 = 0.051$, $b'_2 = 0.795$.

The modelling function (16) is a bit more exact but also more complicated. Its deviation from the experimental data for $t = 5400$ s is less than 0.0015, i.e., twice less than the experimental error.

Thus we wind the modelling functions (15), (16) which can be obtained starting with *a priori* supposition that the coverage profiles can be described by second or third order polynomials of error functions and demanding minimal root-mean-square deviation of these polynomials values from the coverage profiles. This supposition is not necessarily valid for other diffusion systems, e.g., it does not give a constructive way to build approximate modelling profiles for the system discussed in Section 9.

In the following section we present a regular way to calculate modelling functions for any diffusion system using the error function expansion (ERFEX).

7 An algorithm for calculation of modelling functions

We have shown above that erfc functions can be successfully used as construction elements of the modelling functions of coverage profiles at least for a particular diffusion process. Now we shall give a regular way for constructing such functions which has a much more extended application area.

Of course a concrete form of the modelling functions strongly depends on the diffusion system, and we cannot propose a universal method how to obtain the most simple and exact analytical form of an arbitrary concentration curve. Nevertheless, in this section we give an algorithm for calculation of the modelling functions which can be applied to any sufficiently smooth concentration profile in the diffusion zone.

In general case we propose to use ERFEX and search for modelling functions in the form

$$\theta(\xi) = \sum_{i=1}^n A_i \text{erfc}(k_i(\xi - \xi_i)) \quad (17)$$

where ξ_i ($i = 1, 2, \dots, n$) are some fixed values of Boltzmann coordinate, k_i and A_i are parameters which should be specified.

Let $\xi_{i-1} < \xi_i$, or $\xi_1 < \xi_2 < \dots < \xi_n$, then optimal values of k_i lie inside the interval

$$\frac{0.25}{\xi_{i+1} - \xi_i} \leq k_i \leq \frac{1}{\xi_{i+1} - \xi_i}. \quad (18)$$

In particular it is possible to choose the points $\xi_1, \xi_2, \dots, \xi_n$ in a regular way, i.e., with the same distances $\xi_{i+1} - \xi_i$ for all i , and to fix all parameters to be $k_1 = k_1 = \dots = k_n = p$ with some p compatible with (18).

Let $\theta_1, \theta_2, \dots, \theta_n$ be known values of coverage at points $\xi_1, \xi_2, \dots, \xi_n$ and M be a matrix whose elements are $M_{ij} = \text{erfc}(k_i(\xi_i - \xi_j))$. Then parameters A_1, A_2, \dots, A_n are easily found by solving the following system of linear algebraic equations:

$$M_{ij}A_j = \theta_i, \quad i = 1, 2, \dots, n, \quad (19)$$

where summing up over the repeated index j is imposed from $j = 1$ to $j = n$. Equations (19) are nothing but relation (17) considered at points $\xi_1, \xi_2, \dots, \xi_n$.

Let us apply the algorithm to find a modelling function for the diffusion process discussed in Sections 2-6. Consider the results presented in the Appendix for $t = 5400$ s. For simplicity we choose points ξ_1, ξ_2, \dots in a regular way. Namely, we chose in the table selected data corresponding to $x = 0.63, 0.68, 0.73, 0.78, 0.83, 0.88, 0.93, 0.98, 1.03$ and 1.118 (remember that $x_0 = 0.88$), and fix $k_i = 0.7$ for all $i = 1, 2, \dots, n$ ($n = 12$). At that, system (19) is easily solved with using symbolic calculus program MAPLE. As a result we find the following representation for $\theta(\xi)$:

$$\begin{aligned} \theta(\xi) = & -0.0086\text{erfc}(0.7\xi + 3.8865) + 0.0208\text{erfc}(0.7\xi + 3.2333) \\ & -0.0111\text{erfc}(0.7\xi + 2.5801) + 0.0198\text{erfc}(0.7\xi + 1.9269) \\ & +0.0103\text{erfc}(0.7x + 1.2737) + 0.0126\text{erfc}(0.7x + 0.6205) \\ & +0.0242\text{erfc}(0.7\xi - 0.0359) + 0.0328\text{erfc}(0.7\xi - 0.7544) \\ & +0.0385\text{erfc}(0.7\xi - 1.4730) + 0.0211\text{erfc}(0.7x - 2.1915) \\ & -0.0048\text{erfc}(0.7\xi - 2.9000) + 0.0010\text{erfc}(0.7\xi - 3.6285). \end{aligned} \quad (20)$$

This a bit cumbersome formula appears to be very precise; in the interval $-6 < \xi < 6$ it reproduces experimental data (presented in the Appendix) with an accuracy not worse than , moreover, for the majority of experimental points this accuracy is not worse than 0.001. Moreover, using all points given in the Appendix for a fixed time t , it is possible to find "the most exact" modelling functions θ_E whose values simply coincide with the experimental curve. However, taking into account the value of experimental error, such business does not seem to be reasonable.

Notice that using the algorithm with a non-regular distribution of points ξ_i it is possible to find a more simple form of the modelling function:

$$\theta(\xi) = \sum_{i=1}^4 A_i \text{erfc}(R\xi + B_i), \quad (21)$$

where

$$\begin{aligned} A_1 = 0.103, \quad A_2 = 0.234, \quad A_3 = 0.114, \quad A_4 = 0.044, \\ B_1 = -1.87, \quad B_2 = -0.73, \quad B_3 = 1.154, \quad B_4 = 3, \quad R = 0.64. \end{aligned} \quad (22)$$

Being much more simple than (20), function (21) is rather exact too; the corresponding standard quadratic deviation from experimental results is less than 0.003.

8 Calculation of diffusion coefficient

Thus we have at our disposal analytic expressions for a close approximation of coverage profiles. Using them we can calculate the diffusion coefficient $D(\theta)$ by direct integration of equation (12).

First using the simplest modelling function (14) we find $D(\theta)$ for concentrations $\theta < 0.16$, the related values of ξ satisfy $\xi > 0.6$. Substituting (14) into (12) and integrating the resultant expression from $\xi = z > 1$ to infinity, we obtain

$$\begin{aligned} & \frac{2a_1}{\sqrt{\pi}b_1} \left(\operatorname{erf}(b_1\xi)e^{-(b_1\xi)^2} + \frac{1}{\sqrt{2}}\operatorname{erfc}(\sqrt{2}b_1\xi) \right) \Big|_{\infty}^z - \left(\frac{8a_1b_1}{\sqrt{\pi}}\operatorname{erf}(b_1\xi)e^{-(b_1\xi)^2} D \right) \Big|_{\infty}^z \\ &= \frac{2a_1}{\sqrt{\pi}b_1} \left(\operatorname{erf}(b_1z)e^{-(b_1z)^2} + 4b_1^2\operatorname{erf}(b_1z)e^{-(b_1z)^2} D \right) = 0. \end{aligned} \quad (23)$$

Solving (23) for D and using (14) we obtain:

$$D = \frac{1}{4b_1^2} \left(1 + \frac{e^{Z^2}\operatorname{erfc}(\sqrt{2}Z)}{\sqrt{2(1-\frac{\theta}{a_1})}} \right), \quad Z = \operatorname{erfinv} \left(\sqrt{1 - \frac{\theta}{a_1}} \right). \quad (24)$$

where $\operatorname{erfinv}(\cdot)$ is the inverse error function defined by means of $\theta = \operatorname{erf}(\operatorname{erfinv}(\theta))$.

Formula (24) defines the diffusion coefficient D as an explicit function of concentration and is valid for all θ lying in interval $0 \leq \theta < 0.16$.

In an analogous way, i.e., by direct integration of equation (12), it is possible to find the diffusion coefficient D starting with other modelling functions $\theta(\xi)$ found in Sections 6 and 7. The general expression for D is given by the following equation:

$$D(\xi) = \frac{\int_{\xi}^{\infty} z \frac{d\theta(z)}{dz} dz}{2 \frac{d\theta(\xi)}{d\xi}}, \quad (25)$$

which, together with a modelling function for $\theta(\xi)$, determines the diffusion coefficient as a function of θ given in a parametric form.

In contrast to the BM approach, to find the dependence of the diffusion coefficient on concentration we simply need to calculate a definite integral of the *known* function and divide it by the redoubled derivative of (known) function θ with respect to ξ . All these operations are easily handled using, e.g., MAPLE tools.

In Fig. 9 we present a plot of the diffusion coefficient (25) versus the degree of coverage θ given by relation (20). These D values are consistent to within 10-25% with the data obtained in work [6]. However, the maximum at $\theta \approx 0.25$ was not revealed in [6], where the graphical Matano's evaluation of the coverage profiles was applied. This demonstrates that the ERFEX approach provides a more accurate processing of experimental diffusion results.

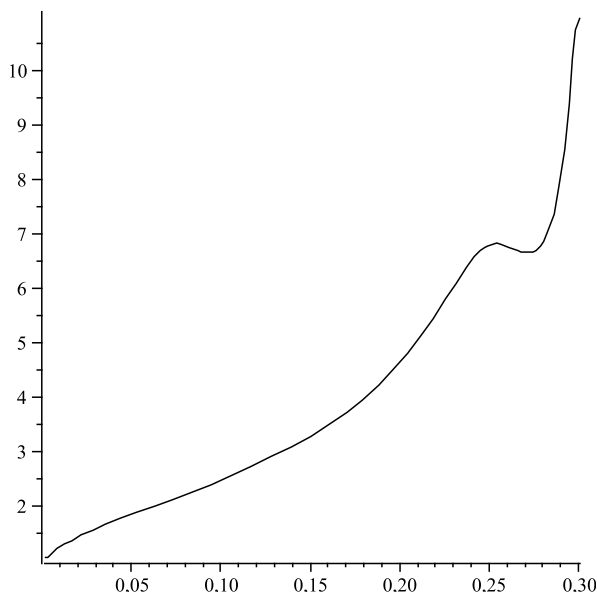


Figure 6: Diffusion coefficient $D(\theta)$ (in units $\text{mm}^2/\text{s} \cdot 10^{-6}$) of Li on Dy-Mo(112) calculated using modelling function (20). $T=600$ K.

9 Modelling functions for coverage profiles of Dy adsorbed on Mo(112)

We have seen that modelling functions (20), (21) give very exact analytic expressions for coverage profiles of Li adsorbed on Mo(112). A natural question arises whether it is possible to find such functions for modelling the profile shapes for other systems.

In this section we apply the ERFEX method to another adsorption system, namely to Dy adsorbed on Mo(112). Experimental data for this system were obtained and discussed in [7]. The related plots of coverage profiles are presented in Fig. 7.

We see that all the profiles recorded in the diffusion process again have a common intersection point this time at $x = 1.69$ which, however, lies out of the initial profile. Their shapes are much more specific than ones given in Fig. 2. There are two zones with a quick change of coverage and three zones where this change is rather slow. These profiles mirror a structural self-organization in the diffusion region, i.e. formation of a series of two-dimensional adsorbate phases which differ from each other by diffusion parameters and mechanisms [7]. Nevertheless, it appears possible to describe these profiles analytically.

First we represent the coverage profiles using the Boltzmann variable $\xi = x/\sqrt{t}$ and setting the reference frame $x_0 = 0$. As a result we conclude that profiles for $t = 2400$ s and $t = 4800$ s became rather close, the mean quadratic deviation of them is less than 0.003. Thus it is possible to describe time evolution of profiles using the approach discussed in Section 3.

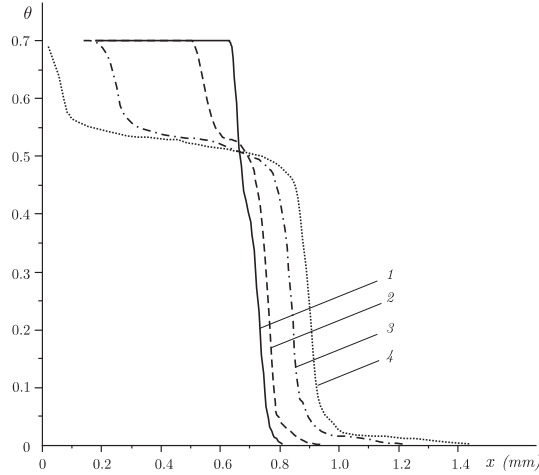


Figure 7: Coverage profile of Dy adsorbed by Mo(112) at T=800 K: initial, $t = 0$ (1) and measured at $t = 360$ s (2), $t = 2400$ s (3), $t = 4800$ s (4) [7].

Using again the ERFEX, we find the following representation for the coverage profile measured at $t = 4800$ s:

$$\begin{aligned} \theta(\xi) = & 0.1673\text{erfc}(2.2124\xi - 6.9912) + 0.06\text{erfc}(0.9434\xi - 3.3962) \\ & + 0.0094\text{erfc}(0.3334\xi - 3.0267) + 0.008\text{erfc}(4.4444\xi - 8.6222) \\ & + 0.006\text{erfc}(2.7778\xi - 3.4722) + 0.0058\text{erfc}(1.2195\xi) + 0.0095\text{erfc}(0.817\xi \\ & + 2.018) + 0.0102\text{erfc}(0.817\xi + 5.1716) + 0.0085\text{erfc}(1.9608\xi + 15.6862) \\ & + 0.062\text{erfc}(2.5\xi + 22.2) + 0.004\text{erfc}(1.9608\xi + 19.2157). \end{aligned} \quad (26)$$

Function (26) is a rather precise approximation of the coverage profile $\theta(\xi)$ at $t=4800$ s; the mean quadratic deviation from the experimental results is less than 0.0015. A plot of the related curves is given by Fig. 8.

We see that ERFEX provides a very good analytical representation for a complicated coverage profile of Dy adsorbed on Mo(112).

10 Discussion

The theory of diffusion is both very old and good developed [14]. Nevertheless, it still contains a lot of unsolved problems which attract attention of numerous investigators.

In the present paper we study three aspects of this theory: using of symmetries in experimental data to describe the time evolution of a diffusion process, searching for a generalized Fick equation which is compatible with these symmetries, and construction of modelling functions to describe concentrations of diffusing substances and calculate the diffusion coefficient.

Like the diffusion theory, the basic branch of mathematics which deals with symmetries, i.e., the theory of continuous groups, is rather old too. It was started by

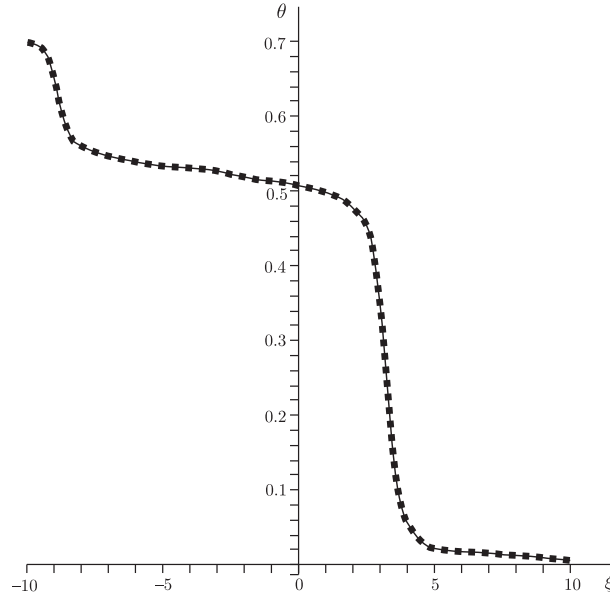


Figure 8: Coverage profile of Dy adsorbed on Mo(112) versus the Boltzmann variable, measured at $t = 4800$ s (full curve) and profile described by function (26) (dotted curve). $T=800$ K.

Sophus Lie around 20 years after appearance of the Fick theory.¹

The classical group analysis and its modern generalizations present effective tools for investigation and applications of symmetries of mathematical models, including diffusion ones. However, to apply these tools directly it is necessary to start with a model formulated in terms of (partial or ordinary) differential equations.²

A specificity of diffusion systems is that in general we do not know evolution equation a priori. Even if there is a cogent argumentation that the process is described by the Fick equation, the dependence of diffusion coefficient on concentration is usually unknown. Thus to apply the Lie analysis it is reasonable *to search for symmetries in experimental data*. And it is the first idea which we use in the present paper.

The second idea is to use erfc functions as a constructive elements of modelling functions for concentration curves, i.e., to apply the ERFEX expansion. There are two origins of this idea: first, a similarity to solutions of the Fick equation with a constant diffusion coefficient, where the erfc function appears very naturally, and secondly, the specific shape of this function curves which seems to be ideal for its use as a "brick" for building typical concentration curves.

Our research is based on a particular diffusion system, i.e., Li adsorbed on Dy-Mo(112), which is well studied and described in papers [5]-[8]. This system represents

¹The background of the continuous group theory was formulated by S. Lie in 1875 and published in 1876 [15]

²Integral, difference and fractional differential equations also are subjects of modern group analysis

many basic features of surface diffusion, and thus we believe that results of our analysis in fact are rather general. A confirmation of this statement was obtained in Section 9, where we considered one more surface diffusion system, i.e., Dy adsorbed on Mo(112).

A precise analysis of the experimental data made it possible to find symmetry transformations (2) which connect experimental curves giving the coverage profiles. Then we apply these symmetries to describe time evolution of the diffusion system and to formulate a possible generalization of the Fick equation, given by relation (13), which keeps invariance with respect to transformations (3). A physical motivation to search for such generalizations is caused by the fact that the values, measured immediately in the experiment to judge of the concentration of diffusing species, are not necessarily in direct proportion to the concentration. Moreover, in some cases we may actually be interested not just in the concentration of particles, but rather in various physical properties connected with it (e.g. electrical conductivity, mechanical strength, optical properties, work function etc.). Suppose that concentration θ and the relevant system property P are related by the dependence

$$\theta = F(P). \quad (27)$$

Substituting (27) into the Fick equation (7) we come to equation (13), where

$$\tilde{D}(P) = D(F(P)), \quad G = \tilde{D} \frac{F''}{F'}, \quad F' = \frac{\partial F}{\partial P}. \quad (28)$$

On the other hand, if a diffusion process is accompanied by dissipation (e.g. due to evaporation or chemical reaction of the diffusing species), the related mathematical model also needs a generalization of the Fick equation by inclusion of the terms depending on $\frac{\partial \theta}{\partial x}$. In order to create a mathematical model of such process which keeps symmetries (3), one should use just the motion equation (13) with $P = \theta$.

We see that the generalized equation (13) appears as a result of rather straightforward considerations and presents an alternative to the generally recognized equation (7). Surely, for the case when θ is a linear function of P and there is no dissipation, equations (13), (28) are reduced to (7).

Use of modelling function for coverage profiles is very convenient for analysis of diffusion processes. These functions are sufficiently exact and can be used for direct calculation of diffusion coefficients starting with the Fick equation.

In the present paper we propose a few modelling functions for coverage profiles of Li adsorbed on Dy-Mo(112). They described experimental data with a high precision, the deviation from experimental data is less than experimental error. Thus the modelling functions present useful tools for both qualitative and quantitative studies of the diffusion systems.

Let us note that calculating the modelling function for small concentrations with higher accuracy (i.e., using all experimental given points) it is possible to find a spike for the diffusion coefficient for small concentrations. The related plot is given by Fig. 9.

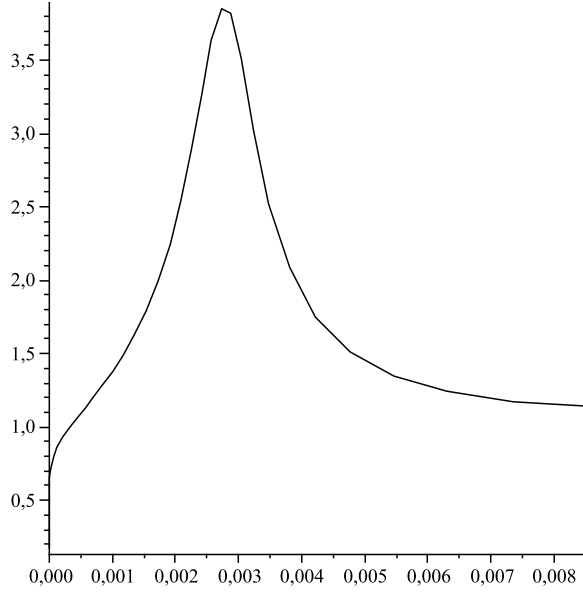


Figure 9: Diffusion coefficient $D(\theta)$ (in units $\text{mm}^2/\text{s} \cdot 10^{-6}$) of Li on Dy-Mo(112) calculated precisely for small concentrations. $T=600$ K.

Notice that the spike in Fig. 9 is indicated for a very small concentrations compatible with the experimental error and so it cannot be treated as well experimentally justified. On the other hand this spike can be observed for all series of experimental data presented by Fig. 2 and also in some other diffusion systems, e.g., in Dy absorbed on Mo(112). Indeed the coverage profile given by Fig. 8 is rather steady at $\xi = 5 - 7$ when $\theta \sim 0.02$ and so the related diffusion coefficient will have a maximum thanks to small value of the derivative $\partial\theta/\partial\xi$.

Concerning interpretation the spike indicated by Figs. 9 and min.-max. presented by Fig. 6 we can mention that the coverage dependence of diffusivity is due to lateral interactions of diffusing atoms and partially also to the specific features of the substrate atomic structure (both intrinsic and caused by defects). The combined action of lateral interactions and surface potential corrugation determines the sequence of phase transitions that occur in the diffusion zone. The phases can differ from one another not only by the diffusion parameters, but also by the diffusion mechanisms (see e.g. a review [8] and references therein). The maxima of diffusivity at low coverage were observed for a number of systems. We attribute this effect to a high mobility of single adatoms. The fast decrease of D with growing coverage may be caused by formation of clusters, whose diffusion mechanisms can be very diversified, but their mobility is generally lower than that of single adatoms. The diffusivity is also rather low in the regions of first-order phase transitions in adlayers. As the coverage grows further and the adlayer becomes increasingly dense approaching a close-packed monolayer, the diffusion takes on a pronounced collective character. In particular,

in the region of commensurate-incommensurate phase transition the diffusion seems to proceed by a relay-race walks of misfit dislocations (topological solitons), which provides a high diffusion rate (a local D maximum). This effect was revealed for many adlayers. For more details refer to papers [8], [16].

Summarizing, we propose a constructive and convenient algorithm (ERFEX) for generating of modelling functions which is valid for arbitrary sufficiently smooth curves not necessarily related to a diffusion process. In particular, using this algorithm and starting with experimental data, it is possible to determine the diffusion coefficient with a higher accuracy than the BM approach and spline approximation. The algorithm can be treated as a specific generalization of the wavelet approach which can be applied to study of diffusions.

Acknowledgments

This work was supported by National Academy of Sciences of Ukraine under Project VC-138.

Appendix

Here we present the table including experimental data obtained for coverage profiles of Li adsorbed by Dy-Mo(112). They are used in the main text to estimate exactness of the modelling functions.

Coverage profiles of Li adsorbed on Dy-Mo(112).

x (mm)	$\theta_1, t = 0$	$\theta_2, t = 1200$ s	$\theta_3, t = 2100$ s	$\theta_4, t = 3600$ s	$\theta_5, t = 5400$ s
0	0.327	0.327	0.327	0.327	0.327
0.20	0.323	0.323	0.324	0.322	0.322
0.40	0.322	0.323	0.319	0.318	0.316
0.48					0.310
0.56					0.300
0.60	0.317	0.316	0.309	0.300	0.291
0.64		0.310	0.305	0.293	0.285
0.68	0.317	0.317	0.295	0.283	0.274
0.72	0.316	0.297	0.288	0.272	0.262
0.76	0.318	0.283	0.270	0.258	0.248
0.80	0.312	0.266	0.253	0.239	0.234
0.84	0.299	0.232	0.221	0.217	0.215
0.88	0.201	0.193	0.194	0.194	0.195
0.90	0.067	0.165		0.177	0.181
0.92	0.036	0.137	0.155	0.159	0.169
0.94	0.025	0.103	0.131	0.144	0.154
0.96	0.013	0.066	0.104	0.122	0.140
0.98	0.010	0.040	0.074	0.105	0.124
1.00	0.008	0.018	0.051	0.081	0.106
1.02		0.012	0.030	0.067	0.091
1.04	0.003	0.008	0.018	0.049	0.077
1.08	0.001	0.003	0.005	0.021	0.047
1.12	0	0.002	0.003	0.009	0.027
1.16	0	0			0.011
1.2	0	0	0	0.001	0.004
1.28					0.001

References

- [1] Fick A 1855 Über Diffusion Ann. Phys., Lpz 170 59
- [2] Matano C 1933 On the relation between the diffusion coefficient and concentration of solid metals Jap. J. Phys 8 109
- [3] Barenblat G 1996 Scaling, Self-Similarity and Intermediate Asymptotics (Cambridge, U.K.: Cambridge University Press)
- [4] Lahtinen J M, Hjelt T and Ala-Nissila T 2000 Diffusive spreading of rodlike molecules on surfaces Surf. Sci. 454-456 598-601

- [5] Naumovets A G, Paliy M V, Vedula Yu S, Loburets A T and Senenko N B 1995 Diffusion of lithium and strontium on Mo(112) *Progr. Surf. Sci.* 48 59-70
- [6] Loburets A T, Senenko N B, Vedula Yu S and Naumovets A G 2002 Experimental study of surface diffusion in metal overlayers on anisotropic metal surfaces, in: *Atomistic Aspects of Epitaxial Growth*, ed. M. Kotrla, N.I. Papanicolaou, D.D. Vvedensky and L.T. Wille (Dordrecht : Kluwer) p 1-19
- [7] Loburets A T, Naumovets A G and Vedula Yu S 1998 Diffusion of dysprosium on the (112) surface of molybdenum *Surf. Sci.* 309 297-304
- [8] Naumovets A G 2005 Collective surface diffusion: An experimentalist's view *Physica A*, 357 189-215
- [9] Olver P 1986 *Application of Lie Groups to Differential Equations* (New York: Springer)
- [10] Ovsiannikov L V 1959 Group properties of nonlinear heat equations *Dokl. Acad.Nauk S.S.S.R.* 123 492
- [11] Knyazeva I V and Popov M D 1986 Group classification of diffusion equations, Preprint 6 of Keldysh Institute of Applied Mathematics (Moscow: USSR Acad. Sci.). See also: *CRC Handbook of Lie Group Analysis of Differential Equations* 1994 ed. N.Ibragimov, Vol 1 (CRC Press) p 171-176
- [12] Nikitin A G 2006 Group classification of systems of non-linear reaction-diffusion equations with general diffusion matrix I. *J. Math. Anal. Appl.* 324, 615-628; Nikitin A G 2007a, II, *ibid.* 332, 666-690; Nikitin A G 2007b Group classification of systems of non-linear reaction-diffusion equations with triangular diffusion matrix *Ukr. Math. J.* 59 395-411
- [13] Samarskii A A, Galaktionov V A, Kurdiumov S P and Mikhailov A P 1987 *Blow up Regimes for Quasilinear Parabolic Equations* (Moscow: Nauka)
- [14] Crank J 1975 *The Mathematics of Diffusion* (Oxford, U.K.: Clarendon Press)
- [15] Lie S 1876 Theorie der Transformationsgruppen *Archiv*, I, 19-58; II, *ibid.* 152-202
- [16] Loburets A T Naumovets A G and Vedula Yu S 1997 Surface diffusion and phase transitions in atomic overlayers. - In: *Surface Diffusion: Atomistic and Collective Processes*, M.C. Tringides (ed.), Plenum, New York, p.509-528
- [17] Naumovets A G Zhang Zh 2002 Fidgety particles on surfaces: How do they jump, walk, group, and settle in virgin areas? *Surf. Sci.* 500 414-436